scientific reports

Check for updates

OPEN

Quantifying fracture roughness effects on coal mine spontaneous combustion through a coupled thermos hydro mechanical model

Guoju Lu✉, Guofei Zhao, Liya Yu, Meihong Zhang & Xiaoli Wang

Accurately predicting and preventing spontaneous coal seam combustion is crucial for mining projects. However, quantitatively assessing the influence of fracture roughness in gas seepage analysis remains highly challenging. To address this issue, we present a novel predictive model for engineering-scale combustion forecasting, which incorporates an interdisciplinary fracture roughness parameter and integrates fracture roughness, heat conduction, chemical reactions, gas pressure, coal-rock stress and deformation, and adsorption–desorption mechanisms to achieve a comprehensive multi-factor coupling in coal seam gas migration. Introducing this parameter provides a more precise representation of gas permeability, heat transfer, and coal seam deformation, thereby enhancing risk assessment accuracy. After rigorous validation, the model was applied to evaluate spontaneous combustion tendencies in the 9th, 14th, and 15th coal seams and their adjacent strata at the Luling Coal Mine in China. Results indicate that the proposed fracture roughness parameter (η) accurately characterizes fracture irregularities, substantially influencing gas flow behaviour and hence spontaneous combustion potential. When η increased from 0.5 to 0.8, the gas proportion in the return airway rose by 7.3%, while coal seam permeability decreased by 51.7%. Under equivalent ventilation durations, higher fracture roughness elevated return airway gas concentrations by up to 16.7%. All these mechanisms were thoroughly and quantitatively evaluated. This study introduces a new quantitative framework for predicting and mitigating coal mine spontaneous combustion, underscoring the pivotal role of fracture roughness in hazard assessment.

Keywords Fracture dynamics, Roughness, Gas flow, Spontaneous combustion, Risk assessment, Fully coupled model

Coal seam spontaneous combustion is an extremely severe disaster in coal mine safety production. It not only causes significant economic losses to coal mining operations but also poses a serious threat to the lives of miners and has long-term adverse effects on the ecological environment[1–4]. Therefore, in-depth research into the mechanisms and influencing factors of coal seam spontaneous combustion is of crucial theoretical and practical significance for the prevention and control of coal mine fires[5–7]. The occurrence of coal seam spontaneous combustion is the result of multiple factors acting in combination, including the coal's material composition, physical properties, and external environmental conditions. Among these, coal-rock fracture behavior, particularly the roughness of fractures, plays a key role in the penetration and diffusion of oxygen within the coal seam. Fracture roughness not only affects the contact area between oxygen and coal, as well as the reaction rate, but also influences the accumulation and dissipation of heat, directly determining the likelihood and development of spontaneous combustion[8–10].

In recent years, the issue of coal seam spontaneous combustion has attracted widespread attention, and numerous scholars have conducted in-depth studies on its mechanisms and prevention measures. The main research directions include the oxidation kinetics of coal, pyrolysis behavior, and analysis of spontaneous combustion tendency[11–13]. Some studies have explored the effects of different coal ranks, coal quality, and particle sizes on the exothermic characteristics of coal oxidation through experimental and theoretical analyses, establishing kinetic models for coal spontaneous combustion. Additionally, in terms of gas flow and heat-mass transfer, researchers have utilized numerical simulation methods to construct multi-field coupling models considering coal seam porosity and permeability, simulating oxygen penetration, coal oxidation reactions,

Department of Safety Engineering, Shanxi Institute of Energy, Jinzhong 030600, China. ✉email: SXgjlu@163.com

and temperature field variations, providing a theoretical basis for predicting spontaneous combustion ignition sites[14–16]. In terms of monitoring and early warning technology, early warning systems based on gas composition analysis, temperature detection, and infrared imaging have been developed to achieve real-time monitoring and risk assessment of coal seam spontaneous combustion[17–19]. These studies provide critical technical support for coal mine safety production. However, despite significant progress in the understanding of coal seam spontaneous combustion mechanisms and prevention technologies, much of the research has focused on the chemical reaction properties of coal, thermodynamic processes, and macroscopic flow behavior. Research on the physical properties of coal-rock fractures, particularly the impact of fracture roughness on oxygen penetration, heat transfer, and the spontaneous combustion process, remains relatively insufficient. Fracture roughness can significantly affect fluid flow and reaction interface characteristics within the coal seam, thereby exerting a substantial influence on the spontaneous combustion process.

The presence and evolution of coal-rock fractures during coal seam spontaneous combustion significantly influence oxygen penetration, heat transfer, and the formation of ignition sources[20–23]. In recent years, research on the impact of fractures on coal seam spontaneous combustion has gradually increased. Using CT scanning technology, researchers can perform three-dimensional reconstructions of the fracture network within coal samples, accurately describing the spatial distribution and morphological characteristics of fractures, thereby providing a microscopic perspective on the fluid flow pathways within the coal seam[24–26]. Additionally, the Discrete Fracture Network (DFN) model has been widely applied to simulate the spatial distribution and connectivity of coal-rock fractures, analyzing their impact on gas flow and heat transfer[27–29]. Fractal theory has also been introduced to fracture research, quantifying the complex geometric features and roughness of fractures, revealing the scale laws and self-similarity of fracture systems[29–31].

In laboratory experiments, oxidation-thermal rise tests with fractured coal samples have been conducted to investigate the effects of fracture parameters (such as width, density, and orientation) on coal spontaneous combustion characteristics[32–34]. These experimental results show that the presence of fractures accelerates oxygen penetration and heat accumulation, significantly lowering the coal's self-ignition temperature. Moreover, some studies have used numerical simulation methods, incorporating real engineering data, to analyze the impact of fracture evolution on coal seam spontaneous combustion risk, providing valuable insights for coal mine fire prediction and prevention. However, despite significant progress in elucidating the role of fractures in coal seam spontaneous combustion, most research remains limited to single-factor analysis, failing to achieve a quantitative understanding of the combined effects of multiple factors, including fracture roughness. Furthermore, laboratory experiments and CT scanning technology are constrained by equipment and scale limitations, making it difficult to comprehensively study fractures at the engineering scale and failing to fully reflect the complexity of actual coal seam fracture systems. Therefore, more extensive and integrated studies are needed to deepen our understanding of the role of fracture roughness in coal seam spontaneous combustion.

To this end, this paper proposes a coal seam spontaneous combustion prediction model suitable for engineering-scale applications. The model integrates multiple factors, including fracture roughness, heat conduction, chemical reactions, gas pressure, coal-rock stress and deformation, and adsorption-desorption processes, establishing a fully coupled numerical simulation system. By comprehensively coupling these key factors, the model can more accurately simulate oxygen penetration, heat transfer, and the spontaneous combustion process within the coal seam. The introduction of fracture roughness effects makes the model more representative of the complex conditions within actual coal seams at the macroscopic scale. This research not only enriches the theoretical study of coal seam spontaneous combustion mechanisms but also provides significant technical support for coal mine fire prediction and prevention, offering important practical implications for ensuring coal mine safety.

Multi-Factor coupled model considering fracture roughness

Energy conduction under multi-factor influence

To capture the effects of rough fractures while coupling convective–conductive heat and mass transfer with adsorption-induced deformation, we adopt the simplifying assumptions[22,23,30,35]: (1) coal deformation is linear-elastic; (2) the gas never attains a supercritical state; (3) gas viscosity is constant; (4) heterogeneity and anisotropy are neglected; (5) the thermo-filtration effect is ignored; and (6) the coal seam comprises a solid matrix and micro-fractures.

Using the volume averaging method, energy balance equations are established separately for the solid phase and the fluid phase, yielding the following[30,35]:

$$(1-\varphi)\cdot(\rho c)_s\frac{\partial T_s}{\partial t}=(1-\varphi)\cdot\nabla\cdot(\lambda_s\nabla T_s)+(1-\varphi)q_s^n \tag{1-a}$$

$$\varphi\cdot(\rho c_p)_f\frac{\partial T_f}{\partial t}+(\rho c_p)_f\mathbf{V}\cdot\nabla T_f=\varphi\cdot\nabla\cdot(\lambda_f\nabla T_f)+\varphi q_f^n. \tag{1-b}$$

Equation (1-a) and (1-b) is for coal matrix solid and gas in coal seam. Where φ is porosity for coal, c is specific heat capacity for solid, the sub s and f is solid and fluid, λ_s is thermal conductivity, q^n is the unit volume of heat generated by a heat source, and $\mathbf{V}\cdot\nabla T_f$ is heat transferred due to convective flow of fluids.

Based on the local thermal equilibrium assumption, we have[35,36]:

$$(\rho c)_m\frac{\partial T}{\partial t}+(\rho c_p)_f\mathbf{V}\cdot\nabla T=\nabla\cdot(\lambda_m\nabla T)+\varphi q_m^n. \tag{2}$$

Where:

$$\begin{cases} (\rho c)_m = (1-\varphi)\cdot(\rho c)_s + \varphi\cdot(\rho c_p)_f \\ \lambda_m = (1-\varphi)\cdot\lambda_s + \varphi\cdot\lambda_f \\ q_m^n = (1-\varphi)\cdot q_s^n + \varphi\cdot q_f^n \end{cases} \tag{3}$$

Considering the impact of fracture roughness on the spontaneous combustion process, rough fractures lead to nonlinear evolution of gas pressure and result in work done by pressure variations. The equation should thus be expressed as:

$$(\rho c)_m \frac{\partial T}{\partial t} + (\rho c_p)_f \mathbf{V}\cdot\nabla T + \frac{1}{\rho}(\cdot\frac{\partial p}{\partial T})_p \cdot T\left(\frac{\partial p}{\partial t} + \mathbf{V}\cdot\nabla p\right) = \nabla\cdot(\lambda_m \nabla T) + \varphi q_m^n. \tag{4}$$

Furthermore, the roughness of fractures induces varying intensities of heat transfer between the fluid within the fractures and the coal seam solid. Therefore, Eq. (1-a) and Eq. (1-b) should be rewritten as:

$$\begin{cases} (1-\varphi)\cdot(\rho c)_s \dfrac{\partial T_s}{\partial t} = (1-\varphi)\nabla\cdot(\lambda_s\nabla T_s) + (1-\varphi)q_s^n + h\cdot(T_f - T_s) \\ \varphi\cdot(\rho c_p)_f \dfrac{\partial T_f}{\partial t} + (\rho c_p)_f\cdot\mathbf{V}\cdot\nabla T_f = \varphi\cdot\nabla\cdot(\lambda_f\nabla T_f) + \varphi\cdot q_f^n + h\cdot(T_f - T_s) \end{cases} \tag{5}$$

Where h is the heat transfer coefficient between the coal seam solid and fluid.

In Eqs. (4) and (5), the fluid pressure is directly affected by fracture roughness. The contribution of fracture roughness to this behavior will be explored in detail in the next subsection.

Non-Isothermal fluid flow considering fracture roughness

In the previous subsection, the influence of fracture roughness on coal-rock temperature was discussed. This is because fracture roughness directly affects gas seepage, which, in turn, leads to the evolution of thermal conduction effects. In this section, a quantitative model will be developed to explore the influence of fracture roughness on gas flow.

In coal seam, the single-factor seepage model considering fracture roughness is given by[37]:

$$k = k_0\cdot\left[1 - \frac{\sqrt{2}\gamma}{a_i}\ln\left(\frac{p}{p_0}\right)\right]^3 \times \frac{[1 - b\,(p-p_0)]}{1 + b\,(p-p_0)}. \tag{6}$$

Where γ is rough fracture height, b represents the ratio of the contact area to the fracture area during fluid flow.

Typically, a model for permeability without considering rough fractures is represented by the cubic law[36,37]:

$$k = k_i\cdot\left[1 - \frac{\sqrt{2}\gamma}{a_i}\ln\left(\frac{p_f}{p_{fi}}\right)\right]^3. \tag{7}$$

Thus, in this study, the fracture roughness parameter is represented by:

$$\eta = \sqrt{2}\cdot\frac{\gamma}{a_i}. \tag{8}$$

Therefore:

$$\begin{matrix} k = k_0\cdot\left[1 - \eta\cdot\ln\left(\dfrac{p}{p_0}\right)\right]^3 \times \dfrac{[1 - b\,(p-p_0)]}{1 + b\,(p-p_0)} \\ k = k_0\cdot\left[1 - \eta\cdot\ln\left(\dfrac{p}{p_0}\right)\right]^3, b = 0 \end{matrix}. \tag{9}$$

Gas seepage through coal-rock can be expressed using Darcy's law:

$$\overrightarrow{q}_g = -\frac{k}{\mu}\nabla p. \tag{10}$$

Where μ is gas viscosity.

The gas flow can be expressed by Forchheimer law[36]:

$$-\nabla p = \frac{k}{\mu}\overrightarrow{q}_g + \rho_g\beta\overrightarrow{q}_g\left|\overrightarrow{q}_g\right| = \frac{k}{\mu}\left(1 + \frac{k}{\mu}\rho_g\beta\left|\overrightarrow{q}_g\right|\right)\overrightarrow{q}_g. \tag{11}$$

Considering fracture behavior and the slip effect, the correction factor for the above equation is as follows:

$$\delta = \frac{1}{1 + \frac{k}{\mu} \cdot \rho_g \beta \left| \overrightarrow{v}_g \right|}. \tag{12}$$

i.e.,

$$\overrightarrow{q}_g = -\frac{k}{\mu}\delta \cdot \nabla p = \frac{k}{1 + \frac{k}{\mu} \cdot \rho_g \beta \left| \overrightarrow{v}_g \right|}. \tag{13}$$

By combining the above equation with Eq. (9), we obtain:

$$\overrightarrow{q}_g = \frac{k_0 \cdot \left[1 - \eta \cdot \ln\left(\frac{p}{p_0}\right)\right]^3}{1 + \frac{k}{\mu} \cdot \rho_g \beta \left| \overrightarrow{v}_g \right|} \times \frac{[1 - b\,(p - p_0)]}{1 + b\,(p - p_0)}. \tag{14}$$

Considering multiple factors such as adsorption-desorption, rock deformation, gas pressure-induced stress, and thermal expansion, the coal seam porosity evolution equation is[38]:

$$\begin{cases} \phi = \dfrac{(1+h)\cdot\phi_0 + \alpha\cdot(T-h)}{1 + \varepsilon_v + (p/K_S) - \varepsilon_w} \\ \dfrac{\phi - \phi_0}{\alpha\cdot(p - p_0)} = \dfrac{\varepsilon_v}{p - p_0} + \dfrac{1}{K_s} - \dfrac{\varepsilon_L P_L}{p(p_0 + P_L)} \end{cases} \tag{15}$$

Where:

$$\begin{cases} \varepsilon_w = p/(P_L + p)\cdot\varepsilon_L \\ h = p_0/K_s + \dfrac{\varepsilon_L \cdot p_0}{(p_0 + P_L)} \end{cases} \tag{16}$$

Where ϕ is porosity during gas flow, ε_v is effective strain caused by multi-factors, α is biot's value, p is gas pressure, K_s is coal particles modulus and ε_L and P_L are the Langmuir constant for strain and pressure.

The gas mass conduction equation under the combined effects of adsorption-desorption, rock deformation, gas pressure-induced stress, and thermal expansion is given by[39,40]:

Combining Eq. (9) with Eq. (18), the mass conduction equation for fluid flow under the influence of fracture roughness and multiple factors is obtained as:

$$M = [\phi + p_a \frac{\rho_c V_L P_L}{p\cdot(P_L + p)^2}]\frac{\partial p}{\partial t} + p\frac{\partial \phi}{\partial t} - \nabla\cdot\left\{\frac{k_0}{\mu}\cdot\left[1 - \eta\cdot\ln\left(\frac{p}{p_0}\right)\right]^3 \times \frac{[1 - b\,(p - p_{0i})]}{1 + b\,(p - p_0)} p\nabla p\right\}. \tag{18}$$

Coal seam mechanics considering fracture dynamics

In coal seams undergoing spontaneous combustion, the total strain tensor of coal-rock can be expressed as:

$$\varepsilon_{ij} = \frac{1}{2}(u_{i,j} + u_{j,i}). \tag{19}$$

Where $u_{i,j}$ is coal displacement component.

Additionally, the mechanical equilibrium of coal-rock can be represented by:

$$\sigma_{ij} + f_i = 0 \tag{20}$$

Where σ_{ij} is stress component, f_i is the coal force component.

In the gas flow and coal seam dynamics process, the effective stress law is expressed as[38,41]:

$$\sigma'_{ij} = G(u_{i,j} + u_{j,i}) - K\varepsilon_c\delta_{ij} + Ku_{k,k}\delta_{ij} - \frac{2G}{3}u_{k,k}\delta_{ij}. \tag{21}$$

Where G is the shear modulus, δ_{ij} is the Kronecker delta.

Therefore, combining the above equations, we obtain:

$$G_{u_i,kk} + \frac{G}{1 - 2\nu}u_{k,ki} - K\varepsilon_{c,i} + f_i = 0. \tag{22}$$

The above equation describes the coal-rock deformation under the influence of gas flow and adsorption-induced expansion forces, which can effectively capture the mechanical characteristics during the coal seam spontaneous combustion process.

It is worth noting that, compared to previously published coal spontaneous combustion evaluation models, this study can quantitatively explore the impact of fracture roughness on coal spontaneous combustion. Moreover, the factors analyzed in this research are highly coupled and interact with each other, as shown in Fig. 1. This is an aspect that related research has been unable to quantitatively characterize.

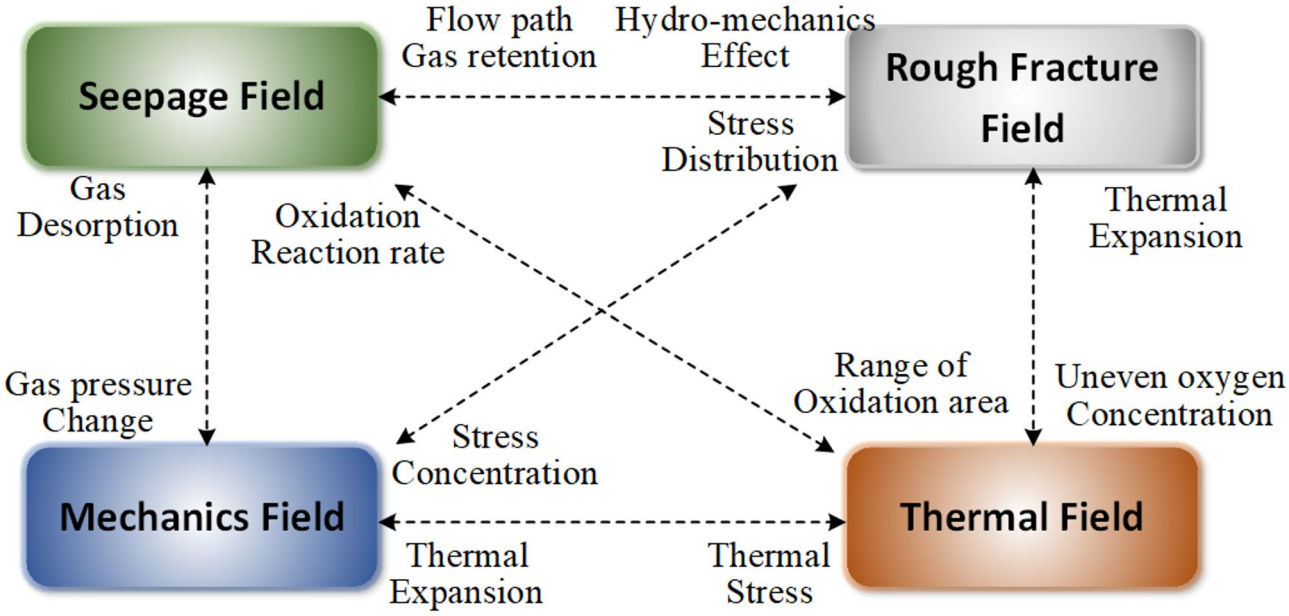

Fig. 1. Interaction of fracture dynamics and other factors in coal spontaneous combustion.

Validation of the proposed model

As the multi-factor analysis model proposed in this study quantitatively explores the contribution of fracture roughness to the coal seam spontaneous combustion process, it is crucial to validate the model's correctness under the effects of fracture roughness and multi-factor coupling before further field evaluations of coal seam spontaneous combustion projects. As demonstrated earlier, this study introduces an innovative multi-field coupling seepage model that quantitatively accounts for fracture roughness in the gas flow process within coal and rock under the influence of multiple factors. Therefore, validating the accuracy of the permeability analysis is essential. Therefore, we simulated the experimental protocol described in references[42,43] using the fracture dynamics model proposed in this study by applying the same vertical (14.5 MPa) and horizontal (9.7 MPa) stresses to the coal sample, saturating it with methane at 6.2 MPa, and subsequently reducing the pore pressure in a stepwise manner down to 0.3 MPa. At each stage, we measured flow rates to estimate the permeability and analysed these values relative to the initial permeability. Our numerical model accurately captured both the mechanical deformation and the adsorption/desorption processes observed experimentally. Moreover, the simulated outcomes closely matched not only the laboratory measurements but also field observations from multiple locations in the San Juan Basin, as illustrated in Fig. 2, thus providing strong evidence of the model's reliability. Consequently, the proposed approach has been thoroughly validated.

After validating the accuracy of the fracture permeability part, it is also important to verify its applicability to the gas-bearing coal seam project under multi-field coupling effects. For this purpose, data from Wang et al.'s field study[40] on gas-bearing coal seams were utilized to validate the model's reliability. Simulations were conducted using the finite element method with COMSOL commercial software. The simulation dimensions, boundary conditions, and gas seepage scenarios for the field project are illustrated in Fig. 3, while the gas seepage data from the field project are presented in Table 1.

The evolution of gas production over time obtained from the model was compared with the field data from Wang et al.[40], as shown in Fig. 4. Some anomalies in the data from the Ma-ti Gorge coal seam may have arisen from monitoring errors, geological fluctuations, or climatic changes. Although our numerical calculations are precise, they do not capture these specific variations, thus the results are presented in an idealized state. This may explain discrepancies between some anomalous data points and our calculated results. Nevertheless, the overall trend of the simulation aligns with theoretical expectations and actual gas production results, thereby validating the reliability of the model.

To rigorously evaluate the agreement between the simulated gas-mining rates and the field observations of Wang et al.[40], the paired data set in Fig. 4 was subjected to an ordinary-least-squares (OLS) regression, with the simulated values regressed against the corresponding measurements. The analysis was performed in OriginPro 2024, and the key statistics are summarised in Table 2.

The regression yields a coefficient of determination $R^2 = 0.88$ and a Pearson correlation coefficient $r = 0.94$ ($p < 0.001$), indicating that 88% of the variance in the field data is captured by the proposed model. The slope (0.95 ± 0.04, 95% CI) is statistically indistinguishable from unity ($t = -1.02$, $p = 0.31$), and the intercept ($2.1 \pm 1.8 \times 10^3$ m^3 d^{-1}, 95% CI) is not significantly different from zero ($p = 0.25$), confirming the absence of systematic bias. Error metrics further demonstrate strong predictive performance: RMSE = 3.8×10^3 m^3 d^{-1}, MAE = 3.1×10^3 m^3 d^{-1}, and MAPE = 3.9%. Collectively, these results substantiate the reliability of the model for practical engineering applications.

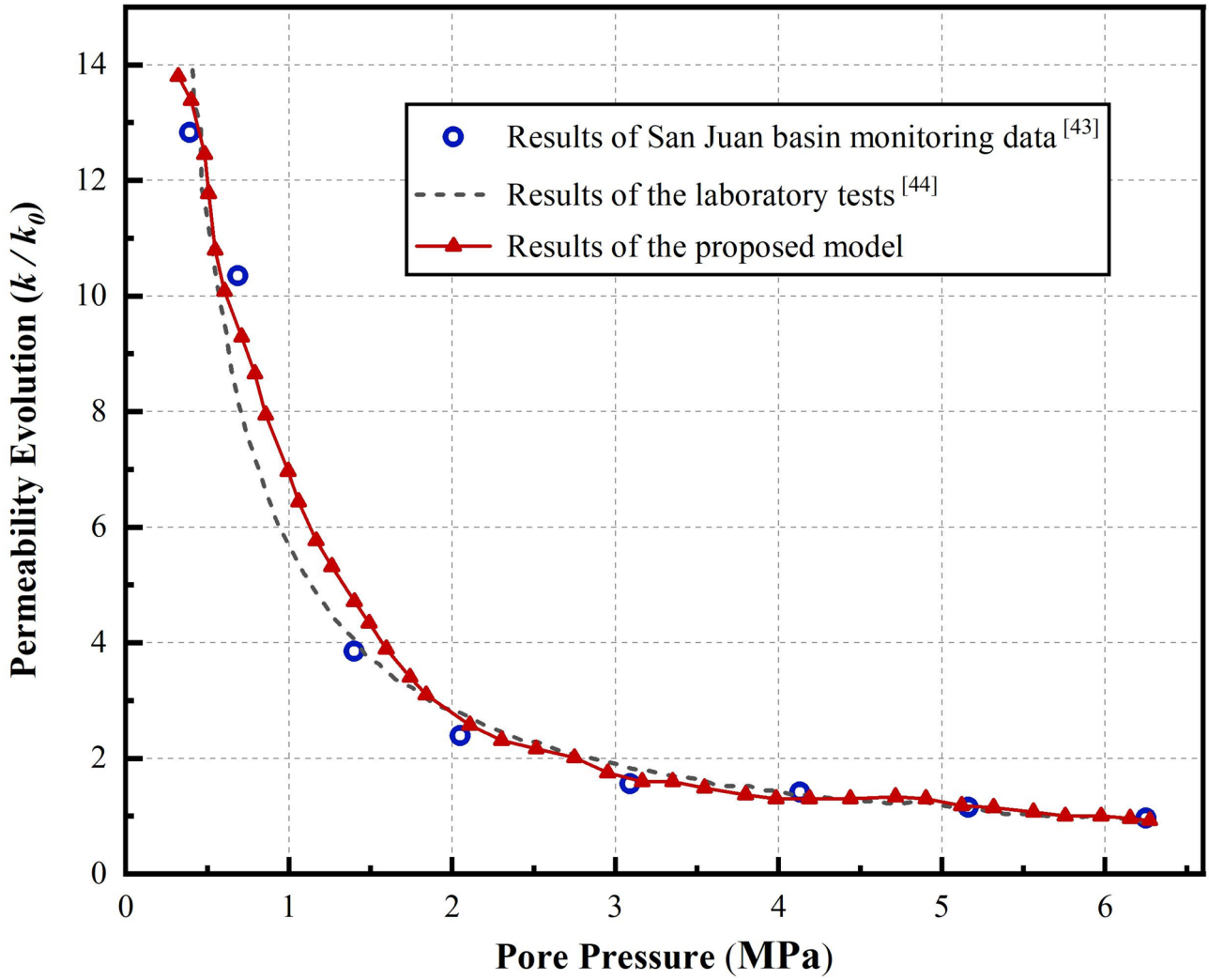

Fig. 2. Model validation by permeability evolution with field data and lab tests.

It is worth noting that Fig. 4 depicts the field simulation of the Ma-ti Gorge coal seam (geometry and parameters derived from Ref. 41; see Fig. 3). Along with the laboratory test in Fig. 2, this simulation corroborates the validity of the governing equations introduced in Sect. 2. After confirming the model's accuracy, we employ it in the subsequent sections to assess field conditions in the Luling Coal Mine.

Numerical experiment: field assessment for china's Luling coal mine

Following comprehensive validation, the multi-factor model formulated in this study—accounting for the influence of fracture roughness—was implemented in a field mining project at China's Luling Coal Mine, focusing on the 9th, 14th, and 15th coal seams and their adjacent coal-rock strata. The dimensions of the coal seams are 160 m×200 m×3 m (9th seam), 140 m×180 m×5 m (14th seam), and 120 m×150 m×3 m (15th seam).

Coal seam dimension in AutoCAD 2024 (Autodesk Inc., San Rafael, CA, USA; https://www.autodesk.com/products/autocad/overview) from proprietary field-survey data collected by the authors at China's Luling Coal Mine. The distribution of the coal seams, their dimensions, as well as the intake and return airways are illustrated in Fig. 5. The primary simulation parameters used are shown in Table 3.

The model developed in this study consists of a system of nonlinear partial differential equations (PDEs) that describe the coupled processes governing coal seam spontaneous combustion. These equations account for heat transfer, mass transport, chemical reactions, and oxygen diffusion, capturing the complex interactions between physical and chemical phenomena involved in coal oxidation and self-ignition. Additionally, the model incorporates fracture dynamics, specifically considering the effect of fracture roughness on the combustion process. This aspect is crucial for understanding the variation in coal seam permeability and oxygen diffusion due to the fractal nature of fracture surfaces, which influences the rate of combustion and self-ignition. Due to the nonlinearity and spatial complexity of the problem, the finite element method (FEM) was employed for numerical solution. The system of PDEs was discretized and solved using COMSOL Multiphysics, which enables the accurate simulation of these complex processes across the coal seam domain. This approach provides a detailed and dynamic representation of temperature evolution, oxygen consumption, and reaction rates, as well

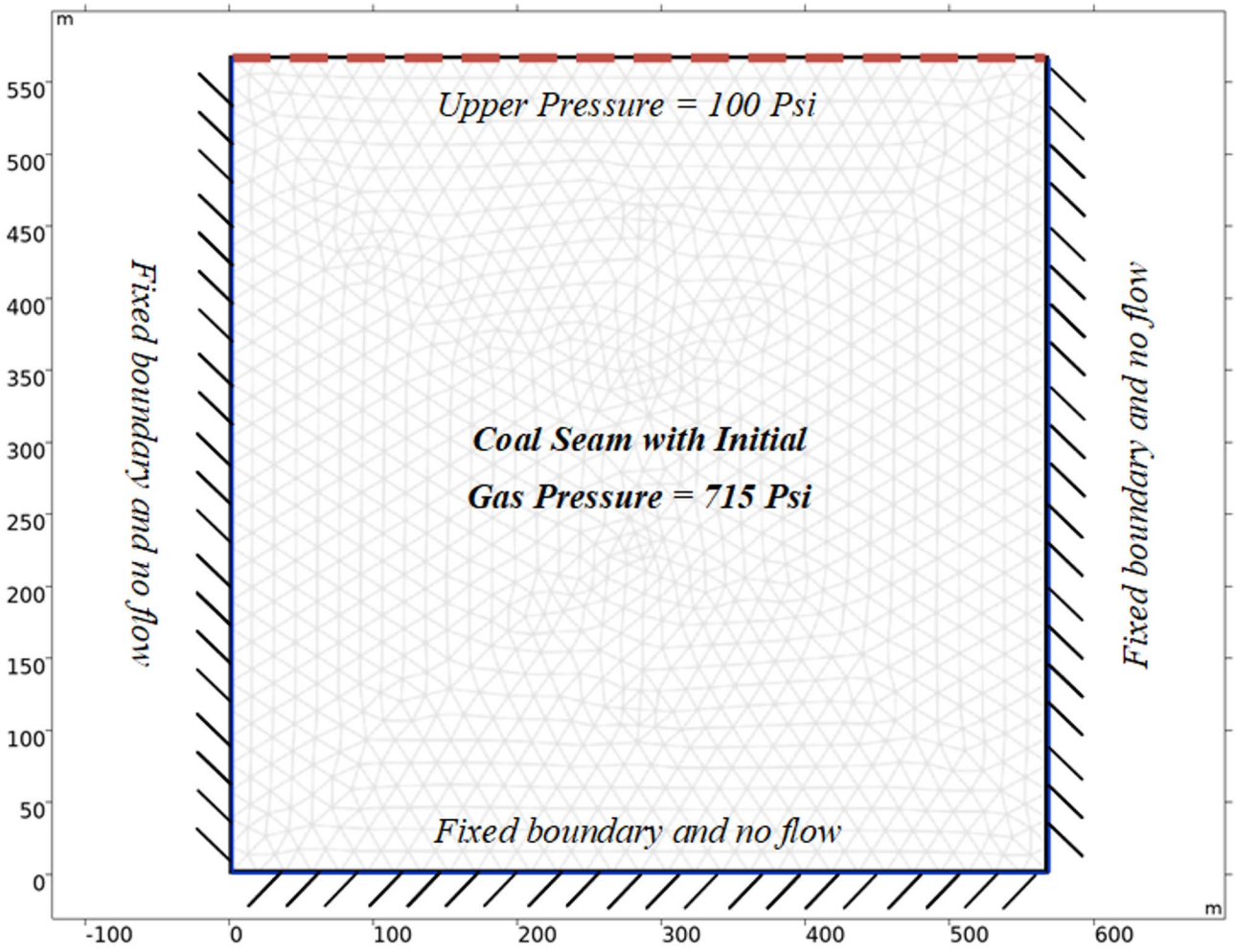

Fig. 3. Schematic diagram of model validation.

Parameter	Value	Unit
Coal density	1250	kg/m³
Coal thermal conductivity	0.2	W/(m·K)
Specific heat capacity of coal	1250	J/(kg·K)
Initial temperature	70	°F
Porosity of the coal seam	0.3	1
Initial oxygen concentration	0.21	kg/m³
Permeability of the coal seam	0.7	mD
Gas pressure in the coal seam	715	Psi
Heat transfer coefficient between coal and air	25	W/(m²·K)
Methane viscosity	1.84×10^{-5}	Pa·s
Poisson's ratio	0.34	1
Gas density	0.717	kg/m³

Table 1. Parameters for model validation.

as the influence of fracture roughness on the self-ignition behavior of coal seams under varying environmental conditions.

Figures 6 and 7 present the distribution of methane and oxygen concentrations in the coal seam under different ventilation times for spontaneous combustion. As described earlier (Fig. 5), the distribution of gas and oxygen concentrations in the coal seam shown in Figs. 6 and 7 aligns closely with actual engineering experience, further validating the accuracy of the fracture dynamics model proposed in this study.

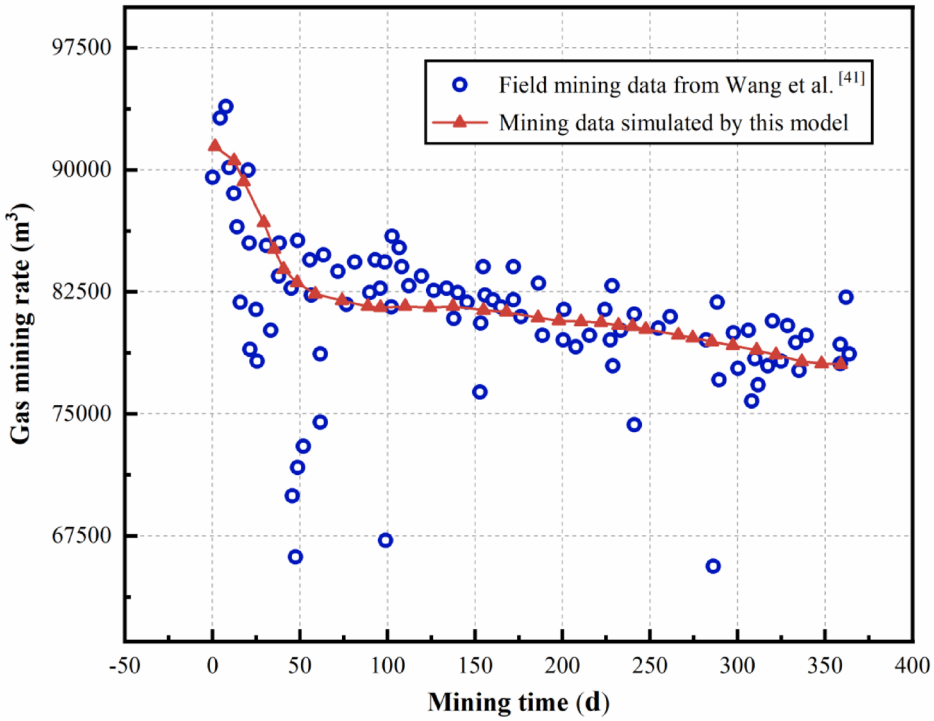

Fig. 4. Model validation with field data from gas-bearing coal seams.

Statistic	Value	95% confidence interval
Slope	0.95	0.91–0.99
Intercept ($m^3\ d^{-1}$)	2.1×10^3	-1.5×10^3 – 5.7×10^3
R^2	0.88	–
Pearson r	0.94	–
RMSE ($m^3\ d^{-1}$)	3.8×10^3	–
MAE ($m^3\ d^{-1}$)	3.1×10^3	–
MAPE (%)	3.9	–

Table 2. Statistical summary of the regression analysis between simulated and field data.

It is noteworthy that although similar results to those in Figs. 6 and 7 can be found in existing literature, the results in this study consider the influence of fracture roughness. This is the main reason for investigating the methane and oxygen concentration distributions in this section. In other words, the results presented in Figs. 6 and 7 provide a comprehensive analysis that fully incorporates the multi-field coupling effects of fracture dynamics, a feature not observed in published studies.

Contribution of fracture roughness on coal seam spontaneous combustion

In the study of spontaneous combustion in coal seams, the distribution of methane and oxygen during ventilation plays a critical role in determining the ignition risk and combustion behavior. The spatial variation in methane and oxygen concentrations directly influences the local chemical reaction rates, and, consequently, the likelihood of self-ignition. Understanding how these gases are distributed within the coal seam is essential for identifying regions at higher risk of combustion. In this context, the roughness of fractures within the coal seam adds significant complexity to the analysis. Fracture roughness impacts the permeability and flow paths within the seam, affecting both the movement of gases and the local oxygen supply. The rougher the fractures, the more irregular the gas flow, which can lead to uneven oxygen distribution and localized accumulation of methane, further enhancing the risk of spontaneous combustion. Therefore, incorporating fracture roughness into the multi-factor analysis is crucial for accurately assessing the stability of coal seams under ventilated conditions, as it influences both gas transport and combustion dynamics in a non-linear manner.

As previously mentioned, the innovative fracture roughness parameter (η) introduced in this study directly reflects the degree of fracture roughness and is fully coupled with the multitude of factors governing gas migration in coal seams. Consequently, as illustrated in Fig. 8, we investigated how this parameter influences the methane concentration in the coal-rock near the return airway. Figure 8 illustrates the evolution of the gas

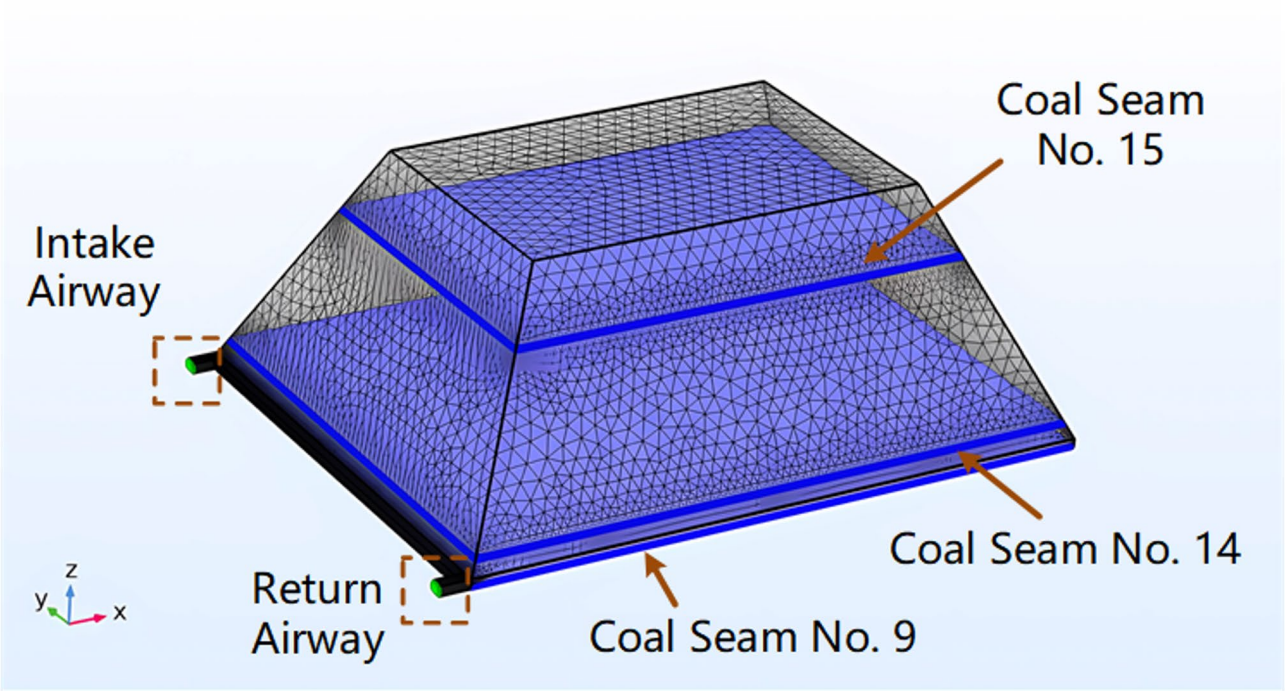

Fig. 5. Simulation diagram of the field coal seam project.

concentration at different distances from the return airway after 10 days of ventilation, under varying values of η (with the horizontal axis representing the intersection between the coal-rock and the return airway at 4 m). As shown in Fig. 8, the fracture roughness parameter η significantly affects ventilation performance. In other words, η directly influences the ventilation efficiency and alters the likelihood of spontaneous combustion in the coal seam. At the furthest point from the return airway ($x = 0$ m), when η increases from 0.5 to 0.8, the proportion of gas in the return airway increases by 7.3%. As mentioned previously, the roughness of the fractures directly leads to changes in the gas flow behavior within the coal seam under multi-factor coupling effects. The fracture roughness parameter η proposed in this study effectively characterizes the roughness of fractures and is directly coupled with the thermo-hydro-mechanical effects in the coal seam.

As outlined in Sect. 2, a larger fracture roughness parameter η corresponds to a rougher fracture surface. In this case, gas seepage becomes more difficult, resulting in less gas being expelled under the same ventilation time. Thus, a lower gas proportion is observed at the outlet under these conditions.

Furthermore, the evolution of coal seam permeability under varying η values was explored. Figure 9 depicts the impact of the fracture roughness parameter η on the permeability at different positions. As seen in Fig. 9, when other parameters remain constant, a larger η leads to a lower permeability. As discussed earlier in Sect. 2, a higher η reflects a rougher fracture surface, making gas seepage more challenging and resulting in a reduced permeability. When η increases from 0.5 to 0.8, the coal seam permeability decreases by up to 51.7%.

To assess the risk of spontaneous combustion in the coal seam, the evolution of gas concentration (mol/m^3) at the return airway entrance was investigated under different ventilation times and η values, as shown in Fig. 10. Figure 10 reveals that, for the same ventilation duration, a larger η leads to a higher gas concentration in the coal seam. When η increases from 0.5 to 0.8, the gas concentration in the return airway increases by up to 16.7%. As noted earlier, a larger η implies a rougher fracture surface and lower permeability. Therefore, a smaller η results in more gas being expelled from the coal seam, leading to better ventilation performance and a lower likelihood of spontaneous combustion.

Importantly, the fracture roughness parameter η introduced in this study is strongly coupled with the coal seam's thermo-hydro-mechanical processes and supports field-scale spontaneous combustion trend analyses. Consequently, the conclusions and models presented here establish a novel methodology for assessing and predicting coal seam spontaneous combustion—an elusive phenomenon in previous literature.

We recognise that the present formulation rests on several assumptions. Nonetheless, it provides the first quantitative insight into how fracture roughness governs coal-seam self-heating. Future work will extend the model to a triple-porosity network—organic pores, inorganic matrix pores, and rough fractures—and will examine a spectrum of porosities alongside fully coupled energy and mass-transfer equations.

Conclusion

This study proposes a multifactor, fully coupled model for predicting coal seam spontaneous combustion, addressing the challenges of quantitatively incorporating microscopic parameters—fracture roughness—into existing assessments. By integrating fracture roughness, gas pressure, coal-rock stress and deformation,

Parameter	Value	Unit
Coal density	1300	kg/m^3
Coal thermal conductivity	0.25	W/(m·K)
Specific heat capacity of coal	1200	J/(kg·K)
Initial temperature	298	K
Oxygen diffusion coefficient	2.1×10^{-5}	m^2/s
Coal-oxygen reaction activation energy	80,000	J/mol
Pre-exponential factor for coal-oxygen reaction	2.5×10^6	s^{-1}
Porosity of the coal seam	0.2	1
Initial oxygen concentration	0.21	kg/m^3
Permeability of the coal seam	1.0×10^{-14}	m^2
Surface area density of coal particles	200	m^2/m^3
Critical temperature for self-ignition	423	K
Coal seam thickness	3.0	m
Gas pressure in the coal seam	101,325	Pa
Heat release rate of coal-oxygen reaction	5.0×10^{-5}	W/kg
Initial moisture content	5.0	%
Heat transfer coefficient between coal and air	25	$W/(m^2 \cdot K)$
Oxygen consumption rate	3.5×10^{-4}	mol/(kg·s)
Thermal diffusivity of coal	2.0×10^{-7}	m^2/s
Latent heat of water evaporation	2,260,000	J/kg
Coal mass fraction of volatile matter	0.35	1
Coal seam ventilation velocity	0.1	m/s
Reaction heat of coal-oxygen reaction	8.0×10^6	J/kg
Adiabatic temperature rise rate	0.02	K/min
Methane Langmuir Volume	25.3	m^3/t
Methane Langmuir Pressure	1.2	MPa
Methane Langmuir Strain	6.5×10^{-4}	1
Oxygen Langmuir Volume	3.2	m^3/t
Oxygen Langmuir Pressure	3.8	MPa
Oxygen Langmuir Strain	8.7×10^{-5}	1

Table 3. Main parameters used in the actual coal seam project.

heat conduction, and chemical reactions, the model offers pivotal technical support for mine fire prediction and prevention, bridging the gap in current models regarding the coupling between fracture roughness and spontaneous combustion processes.

Application of the model to the 9th, 14th, and 15th coal seams and adjacent coal-rock strata at the Luling Coal Mine in China indicates that fracture roughness significantly affects spontaneous combustion. The proposed fracture roughness parameter (η) effectively depicts fracture evolution during coal seam gas flow. When η increases from 0.5 to 0.8 in the return airway, the proportion of gas rises by 7.3%. Meanwhile, the permeability of the coal seam diminishes by as much as 51.7%. Under identical ventilation times, a higher fracture roughness elevates the gas concentration in the return airway by up to 16.7%. These findings suggest that fracture roughness not only governs gas seepage behavior but also serves as a critical factor in spontaneous combustion risk assessment.

Notably, the novelty of this research lies in both the parameterized representation of fracture roughness and the incorporation of thermo-hydro-mechanical effects within a comprehensive numerical framework. Although this study advances the quantitative analysis of spontaneous combustion mechanisms, certain limitations persist. The model presumes relatively uniform coal seam geometry and physical properties across different locations, and future work will refine these assumptions by integrating more geological and mine-specific data for improved calibration.

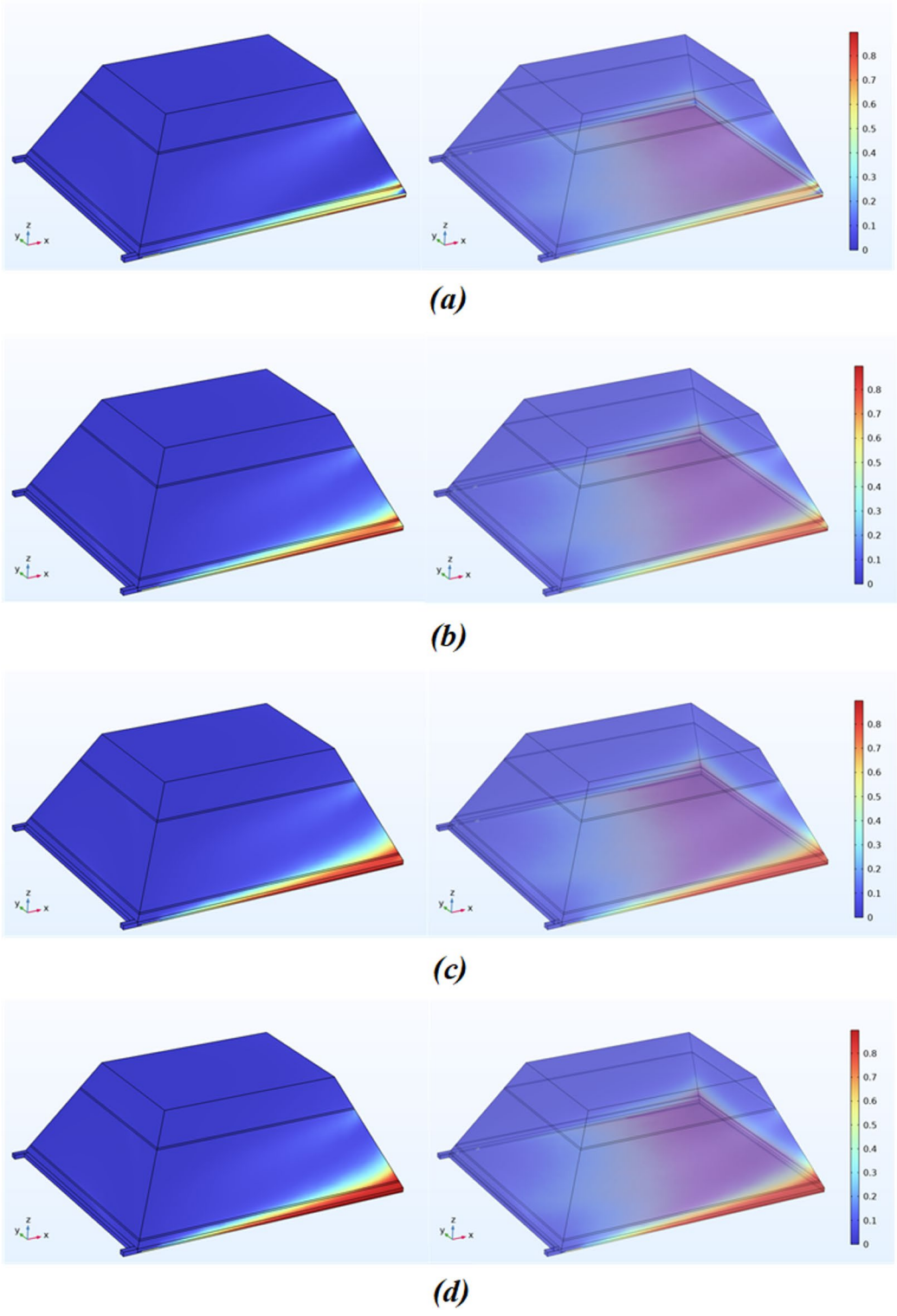

Fig. 6. Methane concentration distribution during ventilation (t = 0.1d, 0.5d, 2d, 5d).

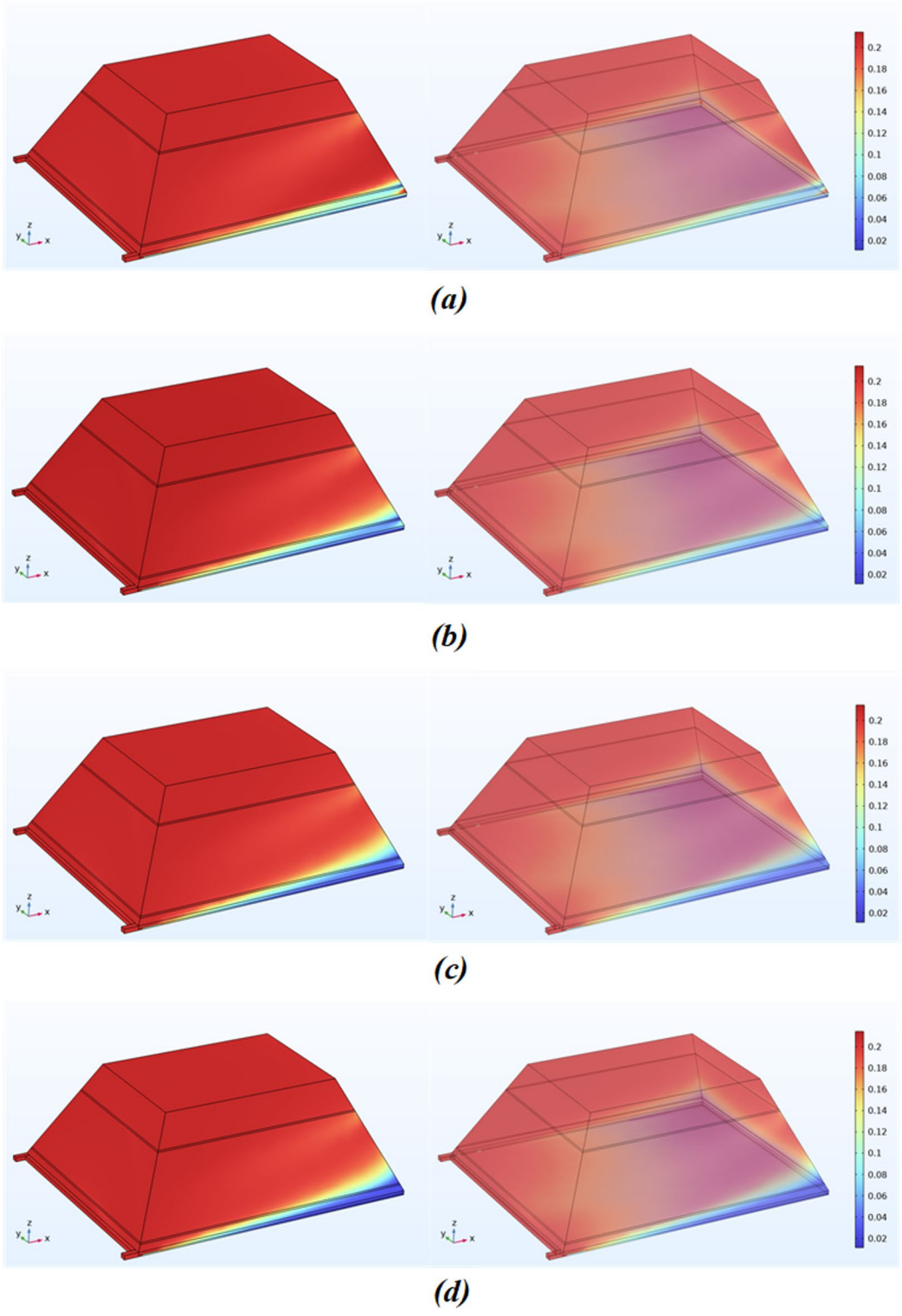

Fig. 7. Oxygen concentration distribution during ventilation (t = 0.1d, 0.5d, 2d, 5d).

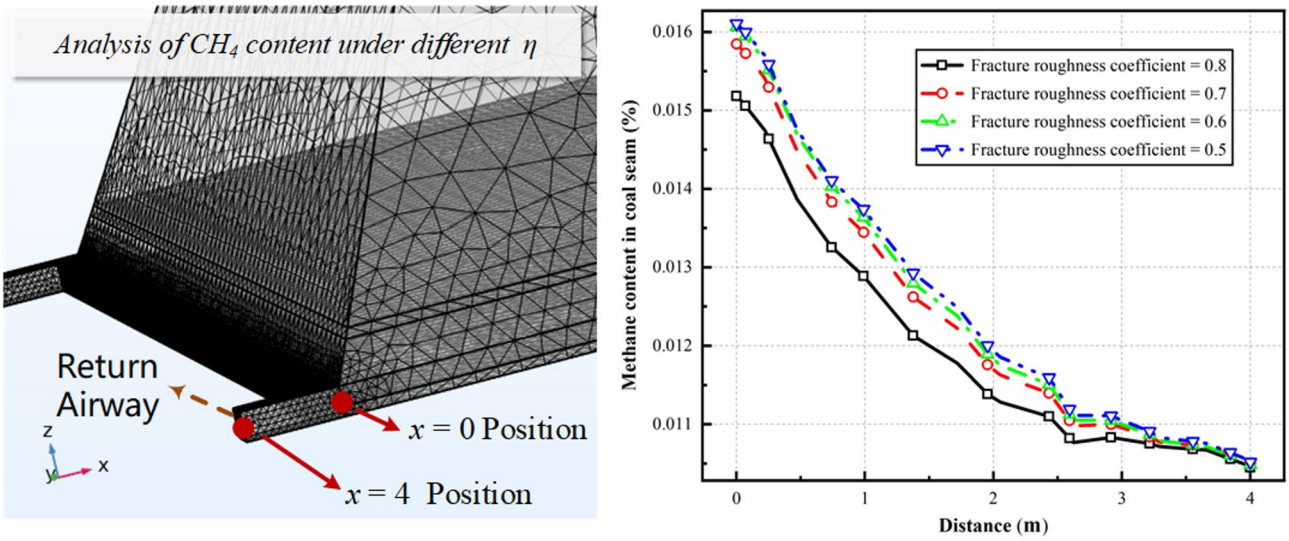

Fig. 8. Influence of fracture roughness on the proportion of gas in coal and rock at various positions.

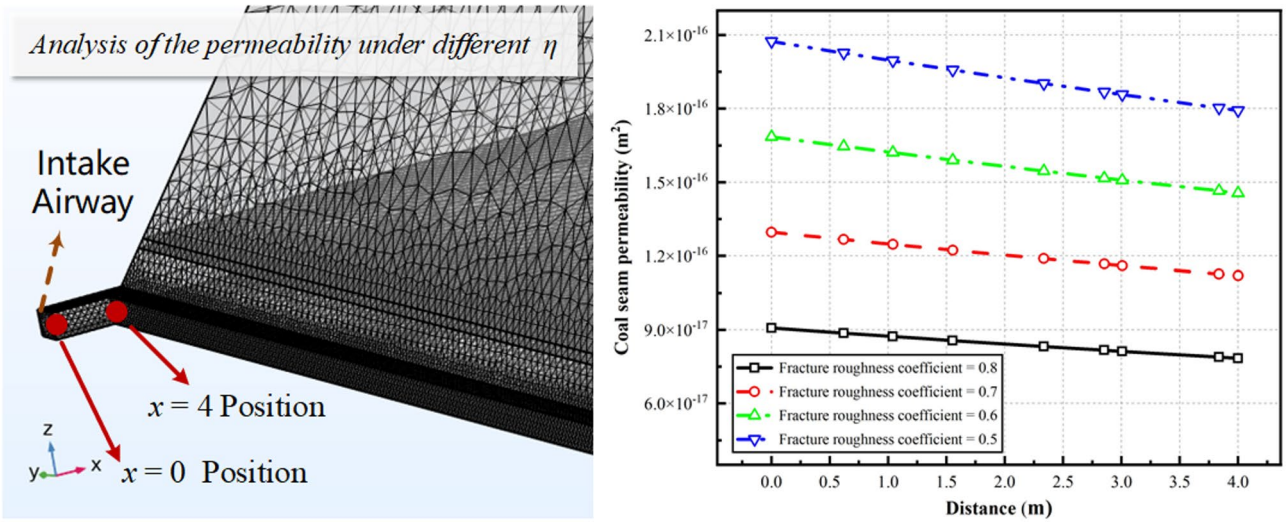

Fig. 9. Influence of fracture roughness on the permeability of coal and rock.

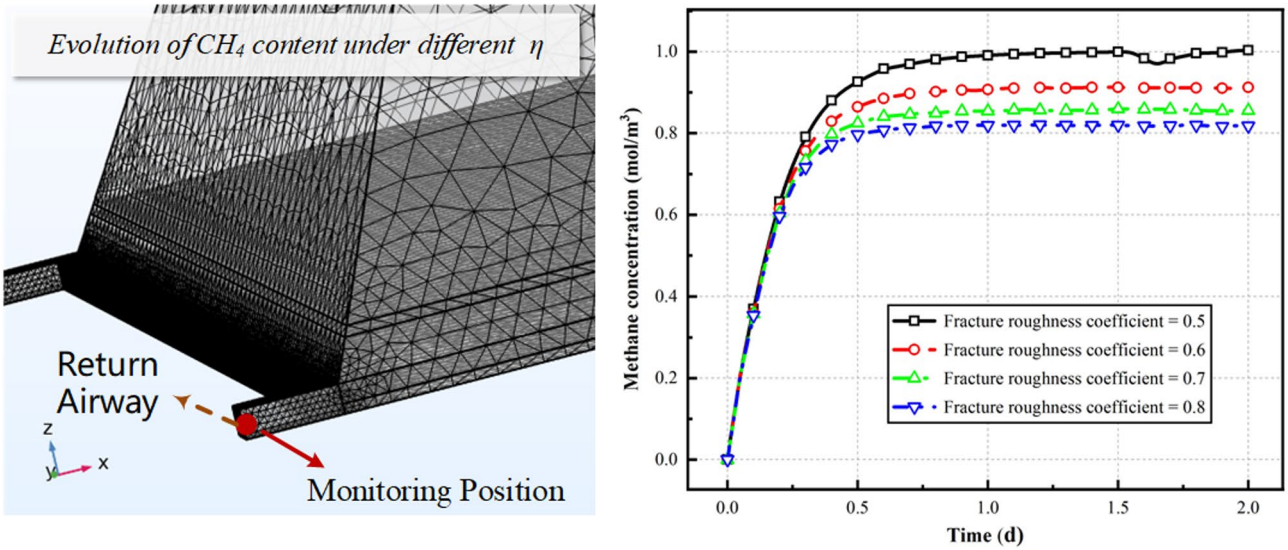

Fig. 10. Influence of fracture roughness on gas concentration in the return airway.

Data availability

The data that support the findings of this study are available from the corresponding author, [Guoju Lu], upon reasonable request.

Received: 20 March 2025; Accepted: 26 June 2025
Published online: 10 July 2025

References

1. Bilen, M., Yılmaz, A. & Rasskazova, A. Determination of gas adsorption properties of Zonguldak Coals. *Solid Fuel Chem.* **59** (2), 127–138 (2025).
2. Singh, R. N., Atkins, A. S. & Shonhard, J. A. A new dimension to management of spontaneous combustion hazard in NSW, Australia. *J. Mines Metals Fuels*, 50. (2002).
3. Ren, Z. et al. Effects of pore size, water content, and oxygen-containing functional groups on oxygen adsorption in bituminous coal. *Sci. Rep.* **13** (1), 10373 (2023).
4. Baris, K., Aydin, H. & Didari, V. Statistical modeling of the effect of rank, temperature, and particle size on low-temperature oxidation of Turkish coals. *Combust. Sci. Technol.* **183** (2), 105–121 (2010).
5. Li, X. et al. Study on condition analysis and temperature prediction of coal spontaneous combustion based on improved genetic algorithm. *AIP Adv.*, **12**(11). (2022).
6. Bilen, M. Online CO monitoring during low temperature oxidation of Zonguldak coals. *Combust. Sci. Technol.*, : 1–19. (2024).
7. Chu, T. et al. Air leakage induced by well developed coal fractures and prevention spontaneous combustion in goaf. *J. Mine Saf. Eng.* **27** (1), 87–93 (2010).
8. Pan, R. et al. Study on the effect of the obstacle on heat transfer oxidation spontaneous combustion characteristic of coal gangue Fracture. *Combust. Sci. Technol.* **193** (15), 2610–2622 (2021).
9. Zhu, H. et al. Research on the influence of fault structure on physical and chemical structure of coking coal during spontaneous Combustion. *Combust. Sci. Technol.*, : 1–29. (2024).
10. Sun, L. et al. Numerical and experimental investigation of coal pillar crushing and spontaneous combustion in shallow and closely spaced coal seams. *Adv. Powder Technol.* **36** (5), 104848 (2025).
11. Baris, K. & Didari, V. Low temperature oxidation of a high volatile bituminous Turkish coal effects of temperature and particle size. (2009).
12. Mandal, S. et al. *A Comparative Kinetic Study between TGA & DSC Techniques Using model-free and model-based Analyses To Assess Spontaneous Combustion Propensity of Indian coals*1591113–1126 (Process Safety and Environmental Protection, 2022).
13. Yang, Q. et al. Study of radon source model in spontaneous combustion Goaf focusing on radon release from coal and Rock. *Combust. Sci. Technol.*, : 1–20. (2024).
14. Tang, Y. et al. Oxidation experiment of coal spontaneous combustion model compounds. *Asian J. Chem.* **25** (1), 441–446 (2013).
15. Han, B. et al. Study on controlling factors and developing a quantitative assessment model for spontaneous combustion hazard of coal gangue. *Case Stud. Therm. Eng.* **54**, 104039 (2024).
16. Said, K. O. et al. On the dependence of predictive models on experimental dataset: A spontaneous combustion studies scenario. *Int. J. Min. Reclam. Environ.* **35** (7), 506–522 (2021).
17. Xu, Y. et al. Risk identification of coal spontaneous combustion in Goaf based on variable weight grey target model. *Energy Sour. Part A Recover. Utilization Environ. Eff.* **44** (2), 5440–5454 (2022).
18. Wang, J., Chen, J. & Liu, M. Theoretical model for spontaneous combustion gangue coarse aggregate concrete filled steel tube stub columns. *J. Constr. Steel Res.* **213**, 108353 (2024).
19. Zhang, H. et al. Application of aging effect model in numerical simulation for predicting spontaneous combustion of coal stockpiles. *J. Therm. Anal. Calorim.* **147** (23), 13847–13860 (2022).
20. Huang, G. et al. Targeted inertization with flue gas injection in fully mechanized caving gob for residual coal spontaneous combustion prevention with CFD modeling. *Energy Sci. Eng.* **8** (11), 3961–3979 (2020).
21. Tang, Z. et al. *Disaster-causing Mechanism and Risk Area Classification Method for Composite Disasters of Gas Explosion and Coal Spontaneous Combustion in Deep Coal Mining with Narrow Coal pillars*132182–188 (Process Safety and Environmental Protection, 2019).

22. Raeini, A. Q., Bijeljic, B. & Blunt, M. J. Generalized network modeling: network extraction as a coarse-scale discretization of the void space of porous media. *Phys. Rev. E.* **96**, (1), 013312 (2017).
23. Palmer, I. Permeability changes in coal: analytical modeling. *Int. J. Coal Geol.* **77** (1–2), 119–126 (2009).
24. Wang, G. et al. *Three-dimensional Modeling and Analysis of macro-pore Structure of Coal Using Combined X-ray CT Imaging and Fractal theory*123104082 (International Journal of Rock Mechanics and Mining Sciences, 2019).
25. Schwartz, F. W., Smith, L. & Crowe, A. S. A stochastic analysis of macroscopic dispersion in fractured media. *Water Resour. Res.* **19**, 1253–1265 (1983).
26. Qiao, Z., Li, C., Wang, Q. & Xu, X. Principles of formulating measures regarding preventing coal and gas outbursts in deep mining: based on stress distribution and failure characteristics. *Fuel* **356**, 129578 (2024).
27. Wang, X. & Cai, M. A DFN–DEM Multi-scale modeling approach for simulating tunnel excavation response in jointed rock masses. *Rock Mech. Rock Eng.* **53**, 1053–1077 (2020).
28. Li, W., Frash, L. P., Welch, N. J., Carey, J. & Meng, M. A simple transient DFN model with stress-dependent fracture permeability for shale gas production. ARMA US Rock Mechanics/Geomechanics Symposium: ARMA; p. ARMA-2020-1723. (2020).
29. Feng, S. et al. Fractal discrete fracture network model for the analysis of radon migration in fractured media. *Comput. Geotech.* **128**, 103810 (2020).
30. Ye, D., Liu, G., Gao, F., Hu, Y. & Yue, F. A fractal model of thermal–hydrological–mechanical interaction on coal seam. *Int. J. Therm. Sci.* **168**, 107048 (2021).
31. Hu, B., Wang, J. & Ma, Z. A fractal discrete fracture network based model for gas production from fractured shale reservoirs. *Energies* **13**, 1857 (2020).
32. He, J. et al. *Effect of Fracture Fluid Flowback on Shale Microfractures Using CT Scanning* (Journal of Rock Mechanics and Geotechnical Engineering, 2023).
33. Guo, Y., Li, X. & Huang, L. Experimental investigation on the sudden cooling effect of oil-based drilling fluid on the dynamic compressive behavior of deep shale reservoirs. *Energy* **282**, 128680 (2023).
34. Fang, X. et al. Stress distribution properties and deformation–fracture mechanisms in hydraulic fracturing of coal. *Fuel* **351**, 129049 (2023).
35. Zhu, W. C., Wei, C. H., Liu, J., Qu, H. Y. & Elsworth, D. A model of coal-gas interaction under variable temperatures. *Int. J. Coal Geol.* **86**, 213–221 (2011).
36. Cao, P., Liu, J. & Leong, Y. K. Combined impact of flow regimes and effective stress on the evolution of shale apparent permeability. *J. Unconv. Oil Gas Resour.* **14**, 32–43 (2016).
37. Zhang, X. et al. Pressure–dependent fracture permeability of marine shales in the Northeast Yunnan area, Southern China. *Int. J. Coal Geol.* **214**, 103237 (2019).
38. Zhang, H. B., Liu, J. S. & Elsworth, D. How sorption-induced matrix deformation affects gas flow in coal seams: A new FE model. *Int. J. Rock Mech. Min. Sci.* **45**, 1226–1236 (2008).
39. Civan, F., Rai, C. S. & Sondergeld, C. H. Shale-gas permeability and diffusivity inferred by improved formulation of relevant retention and transport mechanisms. *Transp. Porous Media*. **86**, 925–944 (2011).
40. Wang, H. et al. Characteristic of stress evolution on fault surface and coal bursts mechanism during the extraction of Longwall face in Yima mining area, China. *J. Struct. Geol.* **136**, 104071 (2020).
41. Ye, D. et al. A multi-field coupling model of gas flow in fractured coal seam. *Adv. Geo-Energy Res.* **5** (1), 104–118 (2021).
42. Gierhart, R. R., Clarkson, C. R. & Seidle, J. P. Spatial variation of San Juan Basin Fruitland coalbed methane pressure dependent permeability: Magnitude and functional form[C]//IPTC 2007: International Petroleum Technology Conference. European Association of Geoscientists & Engineers, : cp-147-00077. (2007).
43. Mitra, A., Harpalani, S. & Liu, S. Laboratory measurement and modeling of coal permeability with continued methane production: part 1–Laboratory results. *Fuel* **94**, 110–116 (2012).

Acknowledgements

This work was supported by 2024 Shanxi Central guide local science and technology development fund project, Hydrodynamic characteristics and feasibility study of long-distance directional hole drainage (No. YDZJSX2024C036) and Shanxi Province Science and Technology Achievement Transformation Guidance Special Project, Transformation of Hard Roof Pressure Relief Technology via Segmented Backward Directional Hydraulic Fracturing (No. 202304021301017).

Author contributions

Guoju Lu: Writing - Original Draft, Software, Methodology, Data Curation. Guofei Zhao: Writing - Review & Editing, Project administration, Investigation. Liya Yu: Formal analysis, Data Curation, Conceptualization. Meihong Zhang: Writing - Original Draft, Visualization, Resources. Xiaoli Wang: Conceptualization, Investigation, Resources.

Declarations

Conflict of interest

The authors declare that they have no known competing financial interests or personal relationships that could have appeared to influence the work reported in this paper.

Additional information

Correspondence and requests for materials should be addressed to G.L.

Reprints and permissions information is available at www.nature.com/reprints.

Publisher's note Springer Nature remains neutral with regard to jurisdictional claims in published maps and institutional affiliations.